Clinical Biomechanics 30 (2015) 940–945

Contents lists available at ScienceDirect

Clinical Biomechanics

journal homepage: www.elsevier.com/locate/clinbiomech

Regional mechanical properties of the long head of the biceps tendon

Christopher W. Kolz [a,b], Thomas Suter [a,c], Heath B. Henninger [a,b,*]

[a] Department of Orthopaedics, University of Utah, Salt Lake City, UT, USA
[b] Department of Bioengineering, University of Utah, Salt Lake City, UT, USA
[c] Department of Orthopaedic Surgery, Kantonsspital Baselland, Liestal, Switzerland

ARTICLE INFO

Article history:
Received 18 May 2015
Accepted 7 July 2015

Keywords:
Biceps tendon
Biceps tenodesis
Biomechanics
Tensile test
Mechanical properties

ABSTRACT

Background: Long head of the biceps tenodesis reliably relieves pain, and restores strength, stability, and normal appearance of the upper extremity in the event of biceps tendinopathies. Regional differences in tendon mechanics may provide surgeons with valuable guidance in the placement of the tenodesis repair construct. The purpose of this study was to compare the mechanical properties of the long head of the biceps tendon in three functional regions of the tendon: intra-articular (proximal), suprapectoral (middle), and subpectoral (distal).
Methods: Uniaxial tensile tests were performed on the long head of the biceps tendon segments to quantify the material and structural properties of the tendon. Material properties were obtained using dogbone-shaped specimens while structural properties were obtained using intact specimens where the clamp boundary conditions simulated the common "gold standard" tenodesis, the interference screw.
Findings: Elastic modulus for the supra- and subpectoral regions were significantly greater than the intra-articular region ($P \le 0.048$). The tensile strength of the subpectoral region tended to be lower compared to all other functional regions ($P = 0.051$). The failure mechanism for intact specimens was similar to that seen for interference screw fixation where tissue failure occurs due to tearing at the bone/tendon/screw interface.
Interpretation: The higher tensile strength of the suprapectoral region compared to the subpectoral region may make this a more desirable location for tenodesis placement based on tissue strength. Similar elastic moduli and structural stiffness between the supra- and subpectoral regions indicate that the construct type may play a bigger role in functional outcomes in relation to construct deformation.

1. Introduction

The long head of the biceps (LHB) tendon is a secondary shoulder stabilizer that contributes to elbow flexion and supination strength, and limits superior humeral head migration (Hwang et al., 2014). In the event of tendonitis, tears, subluxation, or synovitis, LHB tenotomy can reliably relieve pain (Delle Rose et al., 2012; Szabo et al., 2008) but results in decreased strength and abnormal appearance of the upper arm (i.e. "Popeye" deformity) (Chillag and Chillag, 2014; Lim et al., 2011). Biceps tenodesis is an alternative to tenotomy that restores strength, stability, and normal appearance of the upper extremity (Hsu et al., 2011; Wittstein et al., 2011).

Interference screws, suture anchors, and bone tunnels are commonly used long head tenodesis constructs that secure the tendon to the humerus, eliminating pathologic tendon proximal to the construct (Mazzocca et al., 2005; Nho et al., 2010; Richards and Burkhart, 2005; Tashjian and Henninger, 2013). In addition to the repair technique, the location of the repair placement is debated (Johannsen et al., 2013; Patzer et al., 2012; Werner et al., 2014). Subpectoral tenodesis is effective at alleviating pain and is associated with stronger bone for fixation in the humerus, but requires partially detaching and reattaching the pectoralis major to the humerus and can be challenging in arthroscopic repairs (Gilmer et al., 2015; Werner et al., 2015). Suprapectoral tenodesis eliminates the need to detach the pectoralis major by placing the repair proximal to the pectoralis insertion, but presents challenges with "groove pain" and thinner bone stock for hardware fixation (Johannsen et al., 2013; Lutton et al., 2011).

One aspect that may affect the success of tenodesis repair is the mechanical integrity of the tendon. Only one study has investigated the material properties of the LHB tendon (McGough et al., 1996). No studies have examined if regional differences in material or structural properties of the LHB tendon exist. Regional differences in tendon strength or stiffness may provide surgeons with valuable guidance in the selection or placement of the tenodesis repair construct, as well as help define physiologic goals for the strength of tenodesis constructs. In addition, inferior material properties in the proximal tendon could be a factor in why many LHB lesions occur in the intra-articular and biceps pulley regions of the tendon.

* Corresponding author at: University Orthopaedic Center, Orthopaedic Research Laboratory, 590 Wakara Way, Room A0100, Salt Lake City, UT 84108, USA. Tel.: +1 801 587 5207.
E-mail address: heath.henninger@utah.edu (H.B. Henninger).

http://dx.doi.org/10.1016/j.clinbiomech.2015.07.005
0268-0033/

Therefore, the purpose of the present study was to compare the mechanical properties of the LHB tendon for three different functional regions of the tendon. We hypothesized that there would be no differences between the properties of the intra-articular (proximal), suprapectoral (middle), and subpectoral (distal) regions of the LHB tendon. To test the hypotheses, uniaxial tensile tests were conducted to quantify LHB tendon material properties, with metrics including peak stress, elastic modulus, and hysteresis, as well as failure properties of ultimate stress and ultimate strain. To quantify structural properties of the LHB in the setting of biceps tenodesis, intact segments of the tendon were tested with clamp boundary conditions that simulated the common "gold standard" tenodesis, the interference screw. Structural metrics included clamp strain, stiffness, and tensile strength of the segments.

2. Methods

2.1. Specimen preparation

The LHB tendon was harvested from 12 pairs of fresh-frozen human cadaver shoulders with no history of shoulder pathology (10 M, 2 F; mean (SD) age: 58 (6) years [range, 46–67 years]). A board-certified, fellowship-trained orthopaedic surgeon (TS) inspected the tendons upon dissection and found no signs of pathology or rupture. Each tendon was divided into three functional regions designated as the intra-articular (proximal), suprapectoral (middle), and subpectoral (distal) regions (Fig. 1). The lengths of each region were approximated as 30%, 40%, and 30% of the total tendon length, respectively. Segments from one tendon of each pair were punched into dogbone-shaped test specimens to characterize the material properties. The contralateral tendon from the pair remained as intact segments to examine the structural properties of the LHB tendon. Teeth in the clamp simulated the boundary conditions of interference screw tenodesis where the teeth of the screw pinch the tendon against the cortical bone of the humeral shaft (Koch and Burks, 2012). Tendon pairs with at least one tendon less than 70 mm in total length were excluded from testing due to insufficient gauge length for testing all regions. Tendons in each pair were randomized to determine which tendon would be tested in the dogbone configuration.

To determine the cross-sectional area of dogbone segments, a digital caliper was used to measure the width and thickness for each specimen at the midpoint of the gauge length. Cross-sectional area for intact specimens was determined by averaging the area of the proximal and distal ends of each tendon segment. The area of each end was determined by imaging the cross-section using a Prosilica GC1350 Gigabit Ethernet camera (Allied Vision Technologies, Vancouver, BC, Canada) while the tendon rested on a block with a calibration grid affixed in the field of view (Fig. 2). Area was calculated by determining the number of pixels in the cross-section using ImageJ (Schneider et al., 2012) and dividing by the number of pixels in 1 cm^2. Shape was characterized by fitting an ellipse to the outline of the tendon cross-section using ImageJ and measuring the major and minor diameters of the best fit ellipse. Aspect ratio was then determined as the quotient of the major diameter over the minor diameter, where a 1:1 ratio is indicative of a circular cross-section. The distal ends of the tendon segments were used in this procedure, with the exception of the proximal end of the intra-articular tendon segment. A pilot analysis showed similar mean and standard deviations with no significant differences between adjoining ends of tendon.

2.2. Experimental protocol

The experimental protocol was adapted from previous tissue characterization studies (Jackson et al., 2014; Pelled et al., 2012; Thorpe et al., 2012). Tendon segments were clamped in a servo-hydraulic materials testing machine (Instron 1331 Load Frame, Model 8800 controller; Instron Corp., Norwood, MA) equipped with a 1-kN tension-compression load cell (Dynacell Model 2527-130; Instron Corp.) in custom soft tissue clamps (Fig. 3). Three 300-μm fiducial markers were adhered along the gauge length of the tissue using cyanoacrylate. The markers allowed tissue deformation to be monitored with high-resolution video tracking software (DMAS v6.5; Spica Technology Corporation, Maui, HI) using the Prosilica GC1350 camera.

To normalize the initial conditions between specimens of differing size, a preload equivalent to 0.05 MPa stress was applied (stress = preload divided by cross-sectional area of native or dogbone-punched specimen). The tissue was allowed to stress relax for 5 min while maintaining the displacement. The load was then removed and the tissue was allowed to rest for 1 min. The 0.05 MPa pre-stress was reapplied, followed by 10 cycles of loading in a triangle waveform to 8% clamp-to-clamp strain at 1%/s. This displacement kept the tissue below theoretical microstructural failure limits of 5%–6% tissue strain where tissue strain is approximately 50% of clamp strain (Bonifasi-Lista et al., 2005; Provenzano and Vanderby, 2006). Immediately following the cyclic phase, the tendon segments were pulled to failure at 1 mm/s. Throughout testing, the tissue was regularly moistened with 0.9% saline spray.

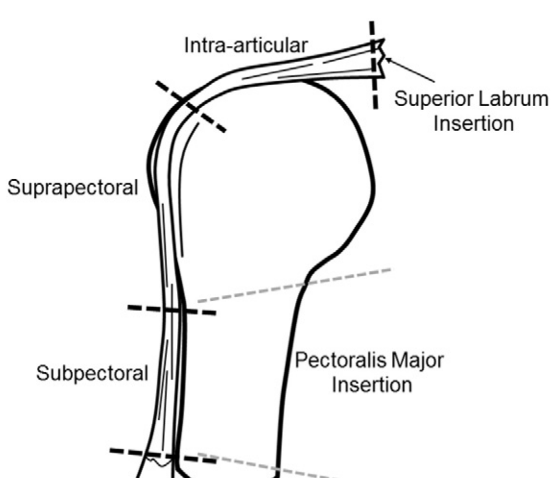

Fig. 1. Demarcation of the three functional regions of the LHB tendon. The intra-articular, suprapectoral, and subpectoral regions were defined by the insertion into the superior labrum, proximal margin of the bicipital groove, proximal edge of the pectoralis major insertion, and musculotendinous junction. This equated to 30%, 40%, and 30% of the total tendon length, respectively.

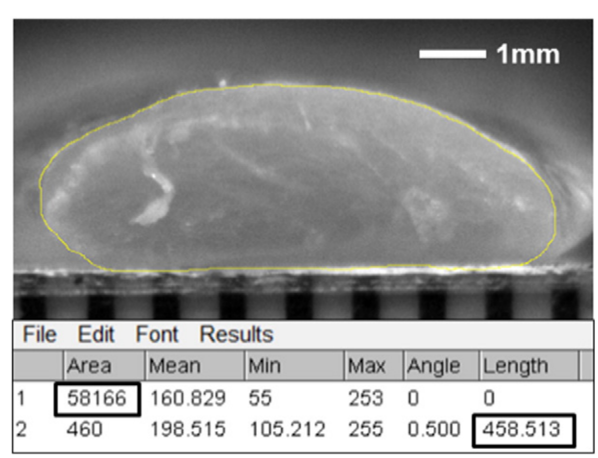

Fig. 2. Sample cross-sectional area calculation using ImageJ. Tendon segments rested on a block with a measurement grid affixed in the field of view. The ends of each tendon segment were imaged and then outlined. Cross-sectional area was determined by converting area in pixels (table line 1) to mm^2 based on pixel length calibration (table line 2, number of pixels in 1 cm).